

Femtosecond laser melting of graphite

D. H. Reitze, X. Wang, H. Ahn, and M. C. Downer

Physics Department, University of Texas at Austin, Austin, Texas 78712

(Received 28 August 1989)

We report the first femtosecond time-resolved measurements of melting dynamics of graphite. A high-reflectivity phase, lasting less than 10 ps, appears *when and only when* the surface is photoexcited above a critical fluence of 0.13 J/cm^2 needed to produce surface damage. The wavelength, polarization, and fluence dependence of time-resolved reflectivity suggest formation of an initial monovalent metallic phase, which transforms within 30 ps to a low-reflectivity phase, similar to that observed in picosecond reflectivity experiments.

Although graphite, like many refractory materials, sublimes when heated adiabatically at subkilobar pressures,¹ several recent experiments²⁻⁶ have shown that graphite temporarily melts when heated rapidly by a short laser or electrical pulse, even at atmospheric pressure. Nevertheless, disagreement remains over the basic material properties of the transient liquid phase of carbon which forms, particularly whether it is a metal or an insulator. The former claim is based on analysis of melt depth and thermal conduction of liquid carbon formed by excitation with 30-ns laser pulses,^{2,3} and on transient electrical conductivity measurements during Ohmic heating by microsecond electrical pulses.⁴ The latter claim is based on time-resolved measurements using 20-ps laser pulses,⁵ which showed decreased surface optical reflectivity following excitation above a well-defined melting threshold, and on a corroborating, albeit controversial,⁴ experiment,⁶ which showed electrically insulating properties of laser-melted graphite functioning as the photoconductive gap material in an optoelectronic switch. Controversy has surrounded the picosecond reflectivity measurements because some authors⁴ have argued that ablated material obscures the liquid surface during or shortly after the pump pulse, causing a reflectivity drop unrelated to formation of an insulating phase. On the other hand, theoretical estimates of ablation rate have been invoked^{5,7} to argue that ablation is negligible at fluences up to several times the melting threshold. Recently, a compromise interpretation has emerged in the form of a joint proposal⁸ that liquid carbon may form in either insulating or conducting form depending on excitation conditions. Indeed both metallic¹ and insulating⁹ liquid carbon have been observed at kilobar pressures under different equilibrium conditions.

In this paper we report femtosecond time-resolved optical reflectivity measurements on highly oriented pyrolytic graphite (HOPG) excited by 90-fs, $0.62\text{-}\mu\text{m}$ laser pulses. For the first several picoseconds following excitation, such experiments probe surface reflectivity before any material ablation is possible, as demonstrated in similar femtosecond experiments on Column IV semiconductors.¹⁰ Our results for these first picoseconds show unambiguously that surface reflectivity at visible wavelengths increases sharply to metallic values as soon as the pump pulse exceeds a well-defined critical fluence of 0.13 J/cm^2 , precisely the fluence at which morphological evidence of opti-

cal damage appears on the sample surface. However, no reflectivity increase occurs with near ultraviolet (4.0 eV) probe pulses, suggesting that the reflectivity edge of the metallic phase lies at or below 4.0 eV. The visible wavelength high-reflectivity phase persists for less than 10 ps, too short to have been resolved in experiments with 20-ps pulses, and cannot be explained as a dense electron-hole plasma in the crystal. However, at later times reflectivity drops below that of the original HOPG, consistent with the result of picosecond measurements.⁵

Our pump-probe technique closely resembles that used in semiconductor melting experiments.¹⁰ 90-fs, $0.62\text{-}\mu\text{m}$ pump pulses from a colliding-pulse dye laser are amplified to millijoule energy at a 10-Hz repetition rate,¹¹ then focused at normal incidence to a $100\text{-}\mu\text{m}$ spot on the sample surface, which is normal to the graphite *c* axis. The photoexcited HOPG surface is probed either at a near normal ($\sim 10^\circ$) or oblique ($\sim 50^\circ$) angle of incidence, by either $0.62\text{-}\mu\text{m}$ pulses, or their second harmonic at $0.31 \text{ }\mu\text{m}$, which have been split from the pump beam, passed through a variable optical delay, and focused to $30\text{-}\mu\text{m}$ diam waist centered on the pump spot. Between each shot the sample was translated $200 \text{ }\mu\text{m}$ to ensure that the pump excited an undamaged region.

Pump fluence at the sample surface was carefully calibrated using pulse energy and pinhole spotsize monitors. Above a critical fluence of 0.13 J/cm^2 , a damage spot appears on the surface. Optical and scanning electron micrographs show the damage morphology to be similar to that described by others.^{2,5} From known material parameters of HOPG,^{3,12,13} we estimate a surface temperature rise of nearly 6000 K at 0.13 J/cm^2 , very close to the high-pressure melting temperature of HOPG. Although only a few microns in diameter at the threshold, the damage spot grows in size according to the Gaussian fluence distribution of the pump pulse.¹⁴

Figure 1(a) shows the first picosecond of the reflectivity response of HOPG probed at near normal incidence with $0.62\text{-}\mu\text{m}$ pulses as pump fluence is varied from 0.13 J/cm^2 to well above the threshold fluence. Just below threshold a small decrease in reflectivity is observed during the pump pulse, which recovers within approximately 200 fs, as illustrated by the data in Fig. 1(b). This signal is caused by the generation, relaxation, and recombination of an electron-hole plasma in the solid graphite. An ex-

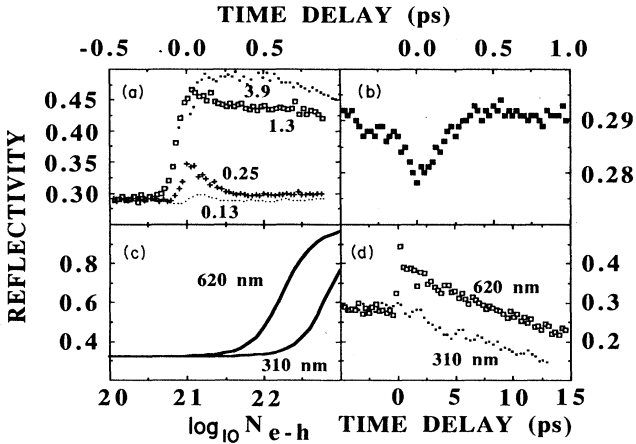


FIG. 1. Femtosecond time-resolved near-normal incidence reflectivity of HOPG for probe wavelength 620 nm (a) following excitation at fluences exactly at damage threshold (0.13 J/cm², dots), and at increasing fluences (0.25, 1.3, and 3.9 J/cm²) above the damage threshold; (b) following excitation just below damage threshold. (c) Normal incidence reflectivity R of HOPG at 620 and 310 nm as a function of optically induced electron-hole pair density N , calculated using Eq. (1) of text. (d) Femtosecond time-resolved normal incidence reflectivity of HOPG excited at 0.7 J/cm², for probe wavelengths 620 and 310 nm. Vertical scales on all panels denote absolute reflectivity.

tensive study of the femtosecond response at this and much lower fluences will be published elsewhere.¹⁵ When pump fluence is increased to exactly 0.13 J/cm², a nearly flat response is observed, as shown by the bottom curve (dots) in Fig. 1(a). Close examination shows a slight drop in reflectivity during the leading edge of the pump, followed by a slight rise during and after the trailing edge. Postmortem analysis of the sample area used in this data run showed that damage occurred for only about half of the shots, because of shot-to-shot energy fluctuations, and that the damage spots which did occur were smaller than the probe spot. Consequently, the data for this curve represents an average of the actual reflectivity responses just below and just above the threshold fluence. As soon as pump fluence is raised slightly above the threshold, however, a sharp increase in reflectivity occurs during the pump pulse. At fluences just above threshold, we observe a partial recovery within ~ 200 fs, followed by a small residual reflectivity increase which persists for nearly 10 ps, as shown by the next highest curve (crosses, $F=0.25$ J/cm²) in Fig. 1(a). As pump fluence is raised further, however, the persistent reflectivity response increases sharply in magnitude, approaching $\frac{5}{3}$ the reflectivity of HOPG, masking the faster signal, and leading to an approximate step function response, as shown by the next higher curve (open squares, $F=1.3$ J/cm²) in Fig. 1(a). At still higher pump fluence, only a slight further increase occurs in the initial reflectivity level, as shown by the top curve (heavy dots, $F=3.9$ J/cm²) in Fig. 1(a). The increasing magnitude of the reflectivity just above the threshold can be attributed to the increasing size of the melt spot compared to the probe spot, and to the increas-

ing initial depth of the melt region compared to the probe depth. In addition spot melting may occur at fluences just above the threshold, causing partial probing of unmelted material. The saturation of the reflectivity rise at high fluences shows that the full probe sees fully melted material.

The precise correlation of surface damage with appearance of a strong transient reflectivity increase at 620 nm provides strong evidence that the latter is caused by melting. Nevertheless, we must address the possibility that generation of an overdense electron-hole plasma in the solid prior to, or during, melting causes or contributes to this reflectivity increase. Although below the melting threshold, generation of carriers always *decreases* reflectivity [Fig. 1(b)], this plasma could *increase* reflectivity if it coincidentally reaches critical density at the melting threshold. This effect can be described by augmenting the dielectric function of unexcited HOPG (Refs. 12 and 13) with a Drude term

$$\epsilon(\omega) = \epsilon_1(\omega) + i\epsilon_2(\omega) - \omega_p^2 / (\omega(\omega + i/\tau)), \quad (1)$$

where $\omega_p^2 = 4\pi Ne^2/m^*$ is the square of the plasma frequency for electron-hole pair density N . The calculated normal incidence reflectivity at 620 and 310 nm as a function of carrier density N is shown by the curves in Fig. 1(c), using reduced effective mass $m^* = 0.5 m$, and Drude relaxation time $\tau = 10^{-14}$ s. A reflectivity increase at 620 nm is expected for $N > 10^{22}$ cm⁻³. At $F = 0.13$ J/cm², linear absorption would generate a carrier density $(1-R)Fa/h\nu = 8 \times 10^{22}$ cm⁻³, neglecting recombination and diffusion during the pump pulse, large enough to increase reflectivity sharply at 620 nm. From this result, generation of an overdense electron-hole plasma probably contributes strongly to the *initial part* (i.e., the first ~ 200 fs) of the reflectivity increase. This conclusion is further supported by (i) the pulsewidth limited rise time of the reflectivity increase, and (ii) the similarity of the partial recovery time constant of ~ 200 fs observed at above threshold fluences [e.g., $F \sim 0.25$ J/cm² data in Fig. 1(a)] to the recovery time constant observed below the damage threshold, suggesting a common origin of this recovery in carrier dynamics.

Nevertheless the reflectivity at *later time delays* (~ 200 fs $< \Delta t < 10$ ps) is inconsistent with the behavior of a solid-state plasma, and can be explained only by melting of the material. Compelling evidence for this conclusion derives from comparing 620-nm with 310-nm reflectivity over this time interval, as shown in Fig. 1(d) for $F = 0.7$ J/cm². With the red probe, we observe the initial 200-fs transient (single data point only on this coarse time scale), a residual reflectivity increase persisting for nearly 10 ps, then a decrease below the reflectivity of the original HOPG. With the uv probe, on the other hand, no reflectivity increase occurs in the first picoseconds, only a relatively slow decrease over 20 ps. The absence of the initial 200-fs transient can be explained by N not reaching the critical density for 310 nm [$N \sim 4 \times 10^{22}$ cm⁻³, see Fig. 1(c)]. When the sample is pumped much harder ($F > 4$ J/cm²), we, in fact, observe this transient very weakly. However, the uv reflectivity for 200 fs $< \Delta t < 10$ ps cannot be reconciled with the model of a solid-state

plasma. First of all, Eq. (1) predicts that such a plasma should *increase* uv reflectivity, albeit only slightly when below critical density, whereas a strong *decrease* is observed. Furthermore, a signal caused by solid-state carriers should recover back toward the reflectivity of unexcited HOPG as the carriers relax and recombine, whereas a monotonic decrease is observed, showing that an irreversible change (melting) has occurred. Finally, the uv reflectivity signal shown in Fig. 1(d) contrasts sharply with our observations of uv reflectivity below the melting threshold. The latter results¹⁵ show a strong uv reflectivity *increase* for $\Delta t > 200$ fs, believed to be caused by heating of the crystal. In addition to this direct experimental evidence, it is highly unlikely that carrier densities as high as several times 10^{22} cm^{-3} (nearly half the π band electron density) could persist as long (~ 10 ps) as the high 620-nm reflectivity signal shown in Fig. 1(d). Our observations below melting threshold¹⁵ show that the Auger recombination coefficient for HOPG is comparable to that of silicon, in which case carrier density would fall below critical density for 620 nm in well under 1 ps. Thus, several independent lines of evidence demonstrate that, apart from the initial 200-fs transient, the increased visible wavelength reflectivity observed above the melting threshold is caused by formation of a disordered metallic phase.

The absence of high reflectivity at 310 nm suggests that the transient metallic phase has a plasma frequency equal to or less than 4.0 eV. Although other Column IV elements form quadrivalent metals in the liquid phase, yielding a plasma frequency of approximately 16 eV, a plasma frequency near 4.0 eV is expected for a monovalent metal. The semimetallic optical and electrical properties of graphite below 8 eV are determined almost entirely by the π -band electrons,^{12,13} which represent only one out of the four valence electrons of carbon. A possible explanation of the observed reflectivity changes then is that intense laser excitation induce structural disordering which pushes the Fermi level to a mid- π -band position, while initially affecting the stronger in-plane sp hybrid σ bonds relatively slightly. Over tens of picoseconds, however, further structural rearrangement could change the chemical bonding structure, causing insulating properties to arise on this time scale.

We now examine the reflectivity response on a longer time scale ($0 < \Delta t < 35$ ps). Figure 2(a) shows the reflectivity of near normally and obliquely incident 0.62- μm probe pulses over the first 35 ps for $F=0.5 \text{ J/cm}^2$. At this fluence ablation is not expected to influence the reflectivity significantly.^{5,7} Indeed analysis of damage spots showed that only a few monolayers of material were removed from the surface. Thus Fresnel equations for a sharp interface should describe the observed reflectivity changes. The three reflectivity curves yield unique values of the optical constants for any time delay. For the unexcited semimetallic HOPG, we obtain $n=2.6$, $k=1.5$, in agreement with published values;^{12,13} at $\Delta t=300$ fs, we obtain $n=1.25$, $k=2.0$, showing increased metallic character; at $\Delta t=35$ ps, we obtain $n=2.2$, $k=0.06$, the reduced k indicating an insulating phase. The ordering of reflectivity values $R_s(\theta=50^\circ) > R(\theta=0^\circ) > R_p(\theta=50^\circ)$ is main-

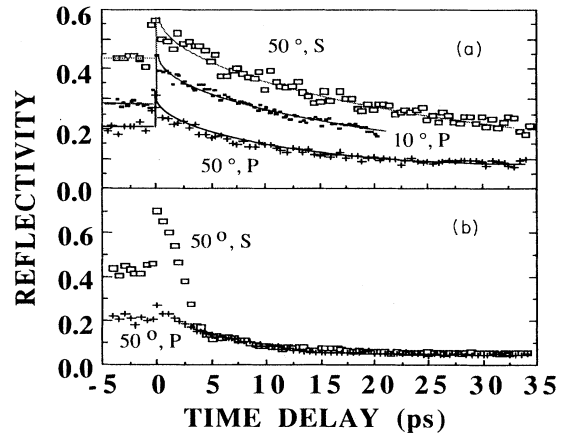


FIG. 2. Femtosecond time-resolved reflectivity of HOPG. (a) Excitation at 0.5 J/cm^2 , probe at 620 nm, comparing 50° incident angle s and p polarized reflectivity, and near-normal incidence reflectivity. Lines through data points are guides to the eye. (b) Excitation at 20 J/cm^2 , probe at 620 nm, comparing 50° incident angle s and p polarized reflectivity.

tained at all time delays, as required by Fresnel's equations for an unobscured, discrete interface. These results therefore support the picture of an initial semimetal-metal transition, followed by a slower metal-insulator transition, with ablation playing a minor role. The steady-state reflectivity, reached in approximately 35 ps, persists for over a nanosecond. For $0.3 < F < 0.7 \text{ J/cm}^2$, there is little change in this steady-state value, roughly half the normal incidence reflectivity of HOPG, consistent with values observed by Malvezzi, Bloembergen, and Huang⁵ using 20-ps pulses of similar fluence and wavelength.

For $F > 0.7 \text{ J/cm}^2$, however, ablation is expected increasingly to influence the reflectivity response, since the surface temperature becomes so high that the equilibrium vapor density approaches the original solid density.^{5,7} Indeed postmortem analysis shows damage spot depths increasing from hundreds to thousands of angstroms in this fluence regime. Figure 2(b) shows the reflectivity response for $F=20 \text{ J/cm}^2$. The initial reflectivity rise is still observed, demonstrating that ablated material still does not rise far enough off the surface in the first few picoseconds to obscure the metallic phase. Within 10 ps, however, strongly fluence-dependent steady-state reflectivity values as low as a few percent are reached. Such low reflectivity can only be explained by strong absorption in a laser-produced plasma. Significantly the initially higher s -polarized reflectivity drops to the same value as the p -polarized reflectivity within 4 ps. Equal reflectivity for obliquely incident s - and p -polarized light cannot occur for a discrete interface, according to Fresnel's equations, further demonstrating that the reflectivity drop is caused by ablation.

In conclusion, we have used femtosecond pump-probe techniques to investigate ultrafast phase transitions in graphite. The major result is observation of a high-reflectivity phase within the first few picoseconds following femtosecond excitation above a critical fluence of 0.13

J/cm², which corresponds precisely to the surface damage threshold. At time delays of tens of picoseconds, however, a lower-reflectivity phase is observed, in agreement with previous picosecond experiments.⁵ These results should stimulate theoretical modeling of the underlying structure and dynamics of the transient phases. It is not yet clear whether the metallic phase observed here bears any relation to the metallic phase observed under nanosecond excitation conditions,^{2,3} or at kilobar pressures.¹ A more ex-

tensive presentation of our results is planned for a future publication.

The authors would like to thank Arthur Moore of Union Carbide for HOPG samples. This work was supported by National Science Foundation Grant No. DMR-8858388, Robert A. Welch Foundation Grant No. F-1038, and the Joint Services Electronics Program Contract No. F49620-89-C-0045.

¹F. P. Bundy, J. Chem. Phys. **38**, 618 (1963).

²T. Venkatesan, D. C. Jacobson, J. M. Gibson, B. S. Elman, G. Braunstein, M. S. Dresselhaus, and G. Dresselhaus, Phys. Rev. Lett. **53**, 360 (1984).

³J. Steinbeck, G. Braunstein, M. S. Dresselhaus, T. Venkatesan, and D. C. Jacobson, J. Appl. Phys. **58**, 4374 (1985).

⁴J. Heremans, C. H. Olk, G. L. Eesley, J. Steinbeck, and G. Dresselhaus, Phys. Rev. Lett. **60**, 452 (1988).

⁵A. M. Malvezzi, N. Bloembergen, and C. Y. Huang, Phys. Rev. Lett. **57**, 146 (1986).

⁶E. A. Chauchard, Chi H. Lee, and C. Y. Huang, Appl. Phys. Lett. **50**, 812 (1987).

⁷N. Bloembergen, in *Beam-Solid Interactions and Phase Transformations, Fall, 1985*, edited by H. Kurz, G. L. Olson, and J. M. Poate, Materials Research Society Symposia Proceedings, Vol. 51 (Materials Research Society, Pittsburgh, 1986), p. 3.

⁸J. Steinbeck, G. Braunstein, J. Speck, M. S. Dresselhaus, C. Y.

Huang, A. M. Malvezzi, and N. Bloembergen, in *Beam-Solid Interactions and Transient Processes, Fall, 1986*, edited by M. O. Thompson, S. T. Picraux, and J. S. Williams, Materials Research Society Symposia Proceedings, Vol. 74 (Materials Research Society, Pittsburgh, 1987), p. 263.

⁹M. T. Jones, National Carbon Research Laboratories, Ohio, Report No. PRC-36, 1958.

¹⁰M. C. Downer, R. L. Fork, and C. V. Shank, J. Opt. Soc. Am. B **2**, 595 (1985).

¹¹W. M. Wood, Glenn Focht, and M. C. Downer, Opt. Lett. **13**, 984 (1988).

¹²E. A. Taft and H. R. Philipp, Phys. Rev. **138**, 197 (1965).

¹³L. G. Johnson and G. Dresselhaus, Phys. Rev. B **7**, 2275 (1973).

¹⁴J. M. Liu, Opt. Lett. **7**, 196 (1982).

¹⁵K. Seibert, H. Kurz, A. M. Malvezzi, and M. C. Downer (unpublished).